Analyst

Dynamic Article Links

Cite this: *Analyst*, 2012, **137**, 2129

www.rsc.org/analyst

**PAPER**

# Graphene oxide integrated sensor for electrochemical monitoring of mitomycin C–DNA interaction†

**Arzum Erdem,*[a] Mihrican Muti,[ab] Pagona Papakonstantinou,*[c] Ece Canavar,[a] Hakan Karadeniz,[a] Gulsah Congur[a] and Surbhi Sharma[c]**

***Received 25th October 2011, Accepted 5th March 2012***
**DOI: 10.1039/c2an16011k**

We present a graphene oxide (GO) integrated disposable electrochemical sensor for the enhanced detection of nucleic acids and the sensitive monitoring of the surface-confined interactions between the anticancer drug mitomycin C (MC) and DNA. Interfacial interactions between immobilized calf thymus double-stranded (dsDNA) and anticancer drug MC were investigated using differential pulse voltammetry (DPV) and electrochemical impedance spectroscopy (EIS) techniques. Based on three repetitive voltammetric measurements of 120 μg $mL^{-1}$ DNA immobilized on GO-modified electrodes, the RSD % ($n = 3$) was calculated as 10.47% and the detection limit (DL) for dsDNA was found to be 9.06 μg $mL^{-1}$. EIS studies revealed that the binding of the drug MC to dsDNA leads to a gradual decrease of its negative charge. As a consequence of this interaction, the negative redox species were allowed to approach the electrode, and thus increase the charge transfer kinetics. On the other hand, DPV studies exploited the decrease of the guanine signal due to drug binding as the basis for specifically probing the biointeraction process between MC and dsDNA.

## 1. Introduction

In the last decade, there has been increasing attention on the binding of small molecules to nucleic acids. Such studies have a key importance for the rational design of more-efficient gene-targeted agents.[1] A variety of small molecules are known to interact reversibly with dsDNA through one of the following three modes: (i) electrostatic interactions with the negatively charged nucleic sugar-phosphate structure; (ii) groove binding interactions; or (iii) intercalations between the stacked base pairs of dsDNA.[2–5]

Analysis of the interfacial biomolecular interaction between DNA-targeted drugs and immobilized DNA probes has a particular role in the rational design of novel DNA-binding drugs and drug screening. The interactions of anticancer drugs with nucleic acids have been studied by numerous physical and biochemical techniques.[6–9] Nuclear magnetic resonance, light scattering studies, viscometry, electric linear and circular dichroism have been applied to provide insight into binding modes, DNA affinity, and base pair selectivity of DNA-binding drugs. However, these techniques mostly address the issues of the binding mechanisms and structural analysis, such as DNA base sequence selectivity, correlation of structure–activity relationships, linkages between the geometry and thermodynamic properties, and influences of substituent modifications on the physical, chemical, and biological properties of the drug–DNA complex. Nucleic acid layers combined with electrochemical transducers have produced a new kind of affinity biosensor capable of rapidly recognizing and monitoring DNA-binding compounds.[10–19] Electrochemical biosensors have been used successfully for a number of applications including monitoring DNA damage, studies of the interactions of DNA with various genotoxic agents (carcinogens, toxins, mutagens, drugs, *etc.*), and also for the detection of specific mutations in DNA sequences. Thus, they potentially offer a faster and cheaper alternative to traditional methods of measuring ligand–DNA interactions.[20–22]

The recent advancements in the development of electrochemical sensors provide novel tools for monitoring biomolecular recognition events at solid surfaces, or solution phases.[10,16,18] Electrocatalytic oxidation of the antiviral drug acyclovir was investigated by Heli *et al.*[17] using a copper nanoparticles-modified carbon paste electrode in combination with cyclic voltammetry (CV) and chronoamperometry techniques. The biomolecular interactions of platinum derivatives anticancer drugs, cisdiamminedichloroplatinum(II) and oxaliplatin with calf

[a]*Ege University, Faculty of Pharmacy, Analytical Chemistry Dept., Bornova, 35100 Izmir, Turkey. E-mail: arzum.erdem@ege.edu.tr; Tel: +90-232-311 5131*

[b]*Adnan Menderes University, Faculty of Science and Arts, Chemistry Dept., 09010 Aydın, Turkey*

[c]*Nanotechnology and Integrated Bio-Engineering Centre, NIBEC, School of Engineering, University of Ulster, Jordanstown campus, UK BT37 OQB. E-mail: p.papakonstantinou@ulster.ac.uk; Tel: +44 (0)28 90368932*

† Electronic supplementary information (ESI) available. See DOI: 10.1039/c2an16011k

thymus dsDNA at the surfaces of a single-walled carbon nanotubes-modified graphite electrode were explored using DPV and EIS techniques by Yapasan *et al.*[18]

Graphene has recently emerged as an interesting material in numerous applications because of its unique electronic and mechanical properties.[23–27] Most of the graphene studies have focused on its physical properties, such as its electronic properties, and these studies have demonstrated some applications in gas[28,29] and pH sensors.[30] The first report concerning graphene electrochemistry and electrocatalytic behaviour was published in 2008 by Shang *et al.*,[31] who used as-grown arrays of vertically aligned graphene nanosheets (GNSs) on silicon as dopamine sensors. Because of their large specific surface area and the good electron transfer ability graphene[31,32] and graphene-modified electrodes can enhance the sensitivity of solid bulk electrodes compared to the unmodified ones.[33,34]

Since the discovery of graphene, a lot of interest has also been focused on GO since it is the most inexpensive precursor for obtaining large quantities of chemically converted graphene. GO, an oxygenated graphene molecule, is formed by extensive chemical oxidation of graphite to form graphite oxide, followed by exfoliation to monolayer-thick sheets by techniques such as sonication or slow-stirring in aqueous solution. Alwarappan *et al.* used reduced graphene oxide (RGO) nanosheets for biosensing applications in order to detect ascorbic acid, dopamine and serotonin.[33] In our earlier study, GO integrated on a single-use graphite electrode was used for the sensitive and selective detection of label-free DNA hybridization related to Hepatitis B virus (HBV) sequences.[35]

MC is an anticancer antibiotic drug, which was isolated from *Streptomyces caespitosus* and is used in clinical anticancer chemotherapy, especially for gastrointestinal cancer. MC has a cytotoxic character that damages normal human cells. Additionally, it was reported that MC can interact with nucleic acids by binding to DNA bases, especially to GC pairs of dsDNA.[36,37]

Earlier studies were focused on monitoring the MC–DNA interaction process by using different electrochemical transducers such as the hanging mercury drop electrode (HMDE), carbon screen-printed electrodes (CSPEs) and carbon paste electrodes (CPEs).[38–41] Perez *et al.* investigated the electrochemical detection of DNA–MC adducts at the hanging mercury drop electrode (HMDE) through their potential controlled interaction at the electrode surface.[41] Karadeniz *et al.* investigated the interaction process in a microemulsion system carrying the anticancer drug MC and DNA by using voltammetric techniques.[39]

Through this work, we demonstrate for the first time the use of the GO integrated electrode as a novel sensor platform for the enhanced monitoring of the biointeraction process between the anticancer drug MC and calf thymus dsDNA under optimum experimental conditions. Firstly, disposable unmodified graphite electrodes and GO-modified ones were tested for the individual detection of drug MC and DNA in order to elucidate the signal enhancement due to the presence of GO at the sensor surface. The effect of MC concentration and DNA concentration has been evaluated on the overall performance of the GO-modified electrode. Then, the surface-confined interaction between MC and DNA was monitored electrochemically by performing DPV and EIS techniques.

## 2. Experimental

### 2.1. Apparatus

All electrochemical measurements were carried out using an AUTOLAB - PGSTAT 302 system supplied with an FRA 2.0 module for impedance measurements and a GPES 4.9 software package (Eco Chemie, The Netherlands). DPV and EIS measurements were carried out. The three electrode system consisted of a disposable pencil graphite electrode (PGE), an Ag/AgCl/KCl reference electrode (BAS, Model RE-5B, W. Lafayette, USA) and a platinum wire as the auxiliary electrode. The EIS measurements were performed in a Faraday cage (Eco Chemie, The Netherlands).

### 2.2. Chemicals

The calf thymus dsDNA, polydAdT, and polydGdC were purchased from Sigma-Aldrich. The stock solutions of dsDNA, polydAdT and polydGdC were prepared in concentrations of 1 mg $mL^{-1}$ with Tris-EDTA (TE) buffer solution (10 mM Tris-HCl, 1 mM EDTA, pH 8.00) and kept frozen (1000 mg $L^{-1}$). More dilute solutions of dsDNA, polydAdT and polydGdC were prepared with 0.50 M acetate buffer solution containing 20 mM NaCl (ABS, pH 4.80).

MC was purchased from Sigma-Aldrich. The stock solution of MC (1000 μg $mL^{-1}$) was prepared using ultrapure water. More diluted solutions of MC varying from 5 to 120 μg $mL^{-1}$ were prepared by using 20 mM Tris-HCl buffer solution (TBS, pH 7.00). Other all chemicals were of analytical reagent grade and they were supplied from Sigma-Aldrich and Merck. All stock solutions were prepared using ultrapure water.

**Graphene oxide (GO).** Graphene oxide (GO) was used for the modification of the disposable electrode. GO nanosheets were produced using the procedure presented in our earlier report[35] that involved extensive sonification of graphite in strong acids.[42] In more detail, 5 g of microcrystalline graphite was sonicated in 120 mL of a 3 : 1 mixture of 18 M $H_2SO_4$ and 17 M $HNO_3$ over 2 h, with a Branson tip sonifier at a power level of 100 W, followed by treatment in a sonication bath for 8 h. The dispersion was allowed to stand at room temperature for 4 days; and the colour of the dispersion turned to purple-brown. After repeated washing by water, the oxide sheets were filtered through a 0.2 mm PTFE membrane. Then, the product was allowed to dry under vacuum overnight and the filtered material had a grayish appearance.

The graphene oxide consisted of a few layers with a typical thickness of 3–5 nm as observed by TEM.[35]

### 2.3. Procedure

Measurements included: (1) the immobilization of the nucleic acid and its detection cycle, (2) MC immobilization and its detection at unmodified and GO-modified disposable PGEs, and (3) electrochemical investigation of the MC–DNA interaction at GO-PGEs. All experiments were carried out at room temperature.

The experimental scheme is presented in Scheme 1.

 

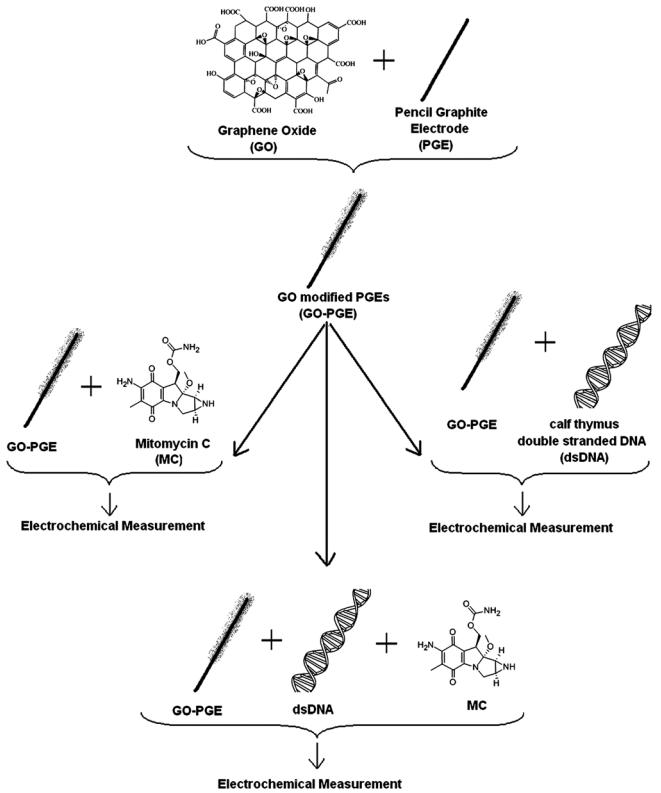


**Scheme 1** Experimental presentations for the modification of pretreated PGEs respectively using GO and DNA, and voltammetric detection of interaction between MC and DNA at the surface of GO-modified PGEs based on the changes at the signals of MC and guanine.

**2.3.1. Preparation of GO solution and GO-modified PGEs.** The required amount of GO was suspended in the organic solvent *N*,*N*-dimethylformamide (DMF), and this mixture was then sonicated for 15 min at room temperature.

PGEs were pretreated by applying a potential of +1.40 V for 30 s in ABS.[16,18] Each pretreated PGE was immersed into vials containing 110 μL of 3000 μg $mL^{-1}$ GO solution for 1 h to form a GO layer at the electrode surface. This easy surface modification of disposable graphite electrodes using GO nanosheets was performed by passive adsorption.[35] Each of the GO-modified PGEs was then allowed to dry for 30 min in an upward position.

**2.3.2. Immobilization of dsDNA onto the surfaces of unmodified PGE and GO-modified PGEs and DNA detection.** The unmodified/GO-modified PGEs were immersed into the vials containing 110 μL of 120 μg $mL^{-1}$ of dsDNA solution in ABS for an hour. The calf thymus DNA was immobilized onto these surfaces by the formation of covalent amide linkages between the carboxyl moieties on the GO surface and the amine group in guanine bases of DNA without any further activation step by using chemical agents *N*-(3-dimethylamino)propyl-*N*′-ethylcarbodiimide hydrochloride (EDC) and *N*-hydroxysuccinimide (NHS).[35] Each of the electrodes was then rinsed with ABS for 10 s before voltammetric transduction as given below.

**2.3.3. MC immobilization onto the surfaces of unmodified PGE and GO-modified PGEs.** The unmodified/GO-modified PGEs were immersed into the vials containing 110 μL of 80 μg $mL^{-1}$ of MC in TBS for 7.5 min. MC was immobilized on GO through the formation of covalent linkages between the carboxyl moieties of GO and amine groups in MC. Each of the electrodes was then rinsed with TBS for 10 s to remove nonspecific bound MC, before voltammetric transduction as given below.

**2.3.4. Interaction of MC with dsDNA at the surface of GO-modified electrode.** For preparation of GO-modified electrodes, the same procedure was followed as given above. The GO-modified PGEs were immersed into the vials containing 110 μL of 120 μg $mL^{-1}$ of dsDNA solution in ABS for an hour. Each of the electrodes was then rinsed with ABS for 10 s before interaction with MC. DNA-immobilized electrodes were immersed into the vials containing 110 μL of 80 μg $mL^{-1}$ MC and allowed to interact for various predetermined durations. Then, each electrode was rinsed with TBS for 10 s before voltammetric transduction.

### 2.4. Voltammetric transduction

After DNA/MC immobilization onto the surfaces of the unmodified PGEs/GO-modified PGEs, DPV measurements were performed in ABS to measure the oxidation signals of MC/guanine by scanning from +0.20 to +1.40 V at a pulse amplitude of 50 mV and a scan rate of 50 mV $s^{-1}$.

The same voltammetric transduction was performed to monitor the changes in the signals of MC and/or guanine before/after the interaction process.

### 2.5. Impedance measurements

The surfaces of unmodified PGEs and GO-modified PGEs were characterized *via* the EIS technique according to the procedure given below. In order to monitor the MC interaction with dsDNA immobilized onto the GO-modified PGE, EIS measurements were also performed at the same conditions.

EIS measurements were performed in the presence of a 2.5 mM $K_3[Fe(CN)_6]/K_4[Fe(CN)_6]$ (1 : 1) mixture, as a redox probe prepared in 0.1 M KCl. The impedance was measured in the frequency range from $10^5$ Hz to $10^{-1}$ Hz in an open-circuit potential value of +0.23 V, *versus* Ag/AgCl with a sinusoidal signal of 10 mV. The respective semicircle diameter corresponds to the charge-transfer resistance, $R_{ct}$, the value of which was calculated using the fitting program of AUTOLAB 302 (FRA, version 4.9 Eco Chemie, The Netherlands).

## Results and discussion

X-Ray photoelectron spectroscopy (XPS) was employed in our study to investigate the oxidation level of GO. The quantification of the data revealed an oxidation content of 19.08 at% and a C : O ratio of 4.24. Fig. 1 shows the C1s peak which is deconvoluted into five components located at 284.49, 285.67, 286.78, 287.90 and 289.00 eV corresponding to $sp^2$ (C=C), hydroxyl (C–OH), epoxide (C–O–C), carbonyl (>C=O) and carboxyl (COOH or HO–C=O) groups, respectively. A ($\pi$–$\pi^*$) shake up satellite peak can also be seen at 290.7 eV.

Firstly, the role of GO was elucidated by comparing the response from 50 μg $mL^{-1}$ calf thymus dsDNA immobilized on

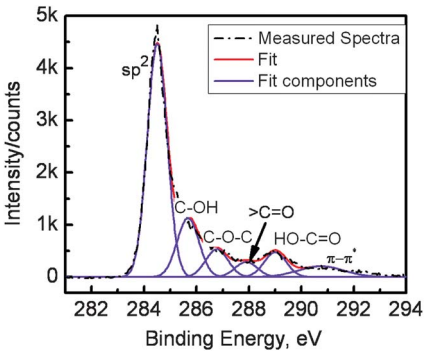


**Fig. 1** XPS spectrum of the graphene oxide (GO).

PGE with and without GO coating. The enhanced guanine oxidation signal was observed at +1.01 V by the GO-modified electrode compared to the unmodified one (Fig. 2). It was found that the response increased approximately by 34.4% with the presence of GO. This increase of guanine signal could indicate that GO enhances the surface area for the binding of nucleic acids.

After DNA immobilization onto the surface of the GO-modified PGEs, the changes in guanine signals were also investigated at various dsDNA concentrations as shown in Fig. 3. A sharp rise in the response was obtained up to 120 μg $mL^{-1}$, with the response leveling off at higher DNA concentrations. Thus, 120 μg $mL^{-1}$ was chosen as the optimum DNA concentration for further studies, indicating the highest DNA coverage at the surfaces of the GO-modified PGEs. Based on three repetitive voltammetric measurements using 120 μg $mL^{-1}$ DNA immobilized onto GO-modified electrodes, the RSD ($n = 3$) was calculated as 10.47%.

A commonly used definition of the DL in the literature of literature of analytical chemistry is that the DL is the analyte concentration giving a signal equal to the blank signal, plus three standard deviations of the blank, *i.e.*

$$y = y_B + 3\varsigma_B \quad (1)$$

The DL was calculated with the aid of the section of the calibration plot close to the origin (show as the inset in Fig. 3)

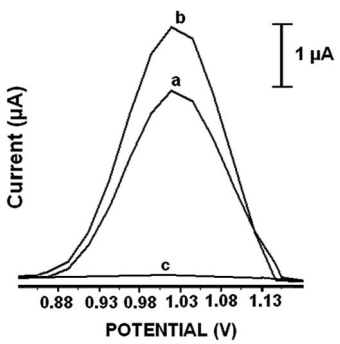


**Fig. 2** DPVs representing the guanine oxidation signals observed by using an unmodified electrode (a) and the GO-modified electrode (b) in the presence of calf thymus 50 μg $mL^{-1}$ dsDNA immobilized during an hour onto the surfaces of electrodes, and (c) the control experiment performed in the absence of DNA by using 3000 μg $mL^{-1}$ GO-modified electrodes.

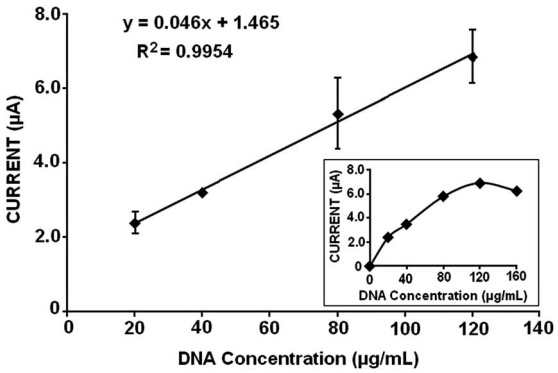


**Fig. 3** Calibration plot presenting the changes of guanine oxidation signal measured in the presence of different concentrations of dsDNA varying from 20 to 120 μg $mL^{-1}$ by using GO-PGEs.

utilizing the regression equation and eqn (1) above.[43] Based on this procedure the DL for dsDNA was calculated as 9.06 μg $mL^{-1}$ with a regression equation: $y = 0.046x + 1.465$ and a regression coefficient ($R^2$) of 0.9954.

In our study, these disposable GO-modified PGEs were used for electrochemical monitoring of anticancer drug–DNA interactions. Under this scope, the anticancer drug MC was chosen as the target compound; this has cytotoxic character, since it can cause damage to normal human cells.[36,37] It is known that MC can interact with nucleic acids by binding to the GC pairs of dsDNA.[44–48]

Before monitoring the surface-confined interaction process, the electrochemical behaviour of MC was investigated at both the unmodified electrode and GO-modified electrode. After the accumulation of 20 μg $mL^{-1}$ MC onto the surfaces of these electrodes, the MC oxidation signals were monitored at +0.86 V by using DPV (shown in Fig. 4). It was shown that an increase of 21.4% was obtained for the MC signal after the GO modification onto the electrode surface. Due to the high density of the carboxyl moieties at the surface of the GO-modified PGE, more MC molecules could accumulate on the surface by the formation of covalent linkage between the carboxyl moieties and the amine groups in MC. It can be concluded that the GO could improve greatly the immobilization capacity and efficiency of the graphite

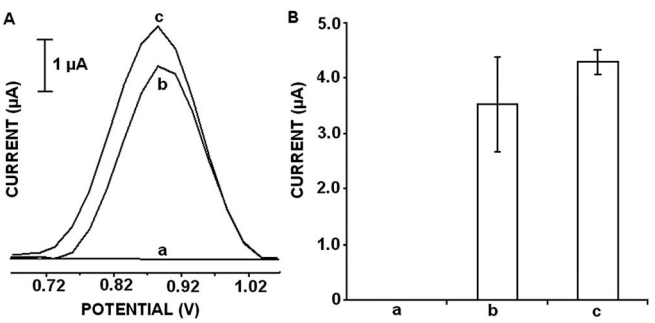


**Fig. 4** (A) DPVs and (B) histograms representing the MC oxidation signals observed by using the unmodified electrode and GO-modified electrode in the absence of MC (a), in the presence of 20 μg $mL^{-1}$ MC immobilized for a period of 7.5 min onto the surface of the unmodified electrodes (b), and 3000 μg $mL^{-1}$ GO-modified electrodes (c).

surfaces.[33–35] In addition, the reproducibility of the GO-modified electrode was found to be much better (RSD % ($n = 3$); 5.24%) than that of the unmodified one (RSD % ($n = 3$); 23.90%).

In order to find the optimum MC concentration on the GO-modified PGE, the changes of MC oxidation signal were monitored for a range of MC concentrations varying from 5 to 120 μg $mL^{-1}$. A sharp increase in the MC signal was obtained for concentrations up to 80 μg $mL^{-1}$ (Fig. S1†), and then the response leveled off till 120 μg $mL^{-1}$ of MC (not shown). Thus, 80 μg $mL^{-1}$ was chosen as the optimum MC concentration for our further study. From the resulting calibration plot of MC (shown inset in Fig. S1†), the detection limit (DL) was calculated as 4.72 μg $mL^{-1}$ according to procedure described by Miller and Miller.[43]

Fig. 5 shows representative voltammograms and histograms for MC and guanine signals observed before and after the surface-confined interaction process at GO-modified disposable electrodes exposed to 80 μg $mL^{-1}$ MC and 120 μg $mL^{-1}$ of dsDNA solutions for different interaction times of 7.5 min (Fig. 5A and B), 15 min (Fig. 5C and D) and 30 min (Fig. 5E and F). The DPV measurements show the oxidation signals of MC and guanine, measured at +0.86 V and +1.01 V respectively. In the case of the 7.5 min interaction time, a gradual decrease of 31.3% and 94.3% was obtained for MC and guanine signals respectively (shown in Fig. 5A and B, a to a′ and b to b′). For a prolonged interaction time of 30 min, the decrease of the signals was found as 58.1% for MC, and 97.2% for guanine (shown in Fig. 5E and F, a to a′ and b to b′). A similar significant decrease of the guanine signal was explained in earlier reports[38–40,44] by the shielding of oxidizable groups of electroactive DNA bases following the surface-confined interaction of the drug within dsDNA.

Before and after the interaction process of MC with the polydAdT-modified electrode, or polydGdC-modified electrode, the changes of the MC oxidation signal were also monitored in order to prove the preferential interaction of MC for the G–C sites compared to the A–T sites of the DNA (shown in Fig. S2†).

Similar to the results shown in Fig. 5A, a to a′, a 37.5% decrease of the MC signal was also recorded for the MC–polydGdC interaction time of 7.5 min (shown in Fig. S2a to c†). By contrast, there was only a 1.4% decrease for MC signal in the case of the MC–polydAdT interaction (shown in Fig. S2a and b†). Weaver and Tomasz[48] reported that the 2-amino group of the guanine residues in synthetic polyribonucleotides are the major covalent binding sites with the antibiotic MC. Later, Paz *et al.*[49] reported that DNA damage is generated from mono- and bi-functional alkylation of the guanine residues by MC leading to MC–guanine monoadducts and MC–guanine bisadducts; the latter constitute DNA interstrand and intrastrand cross-links,

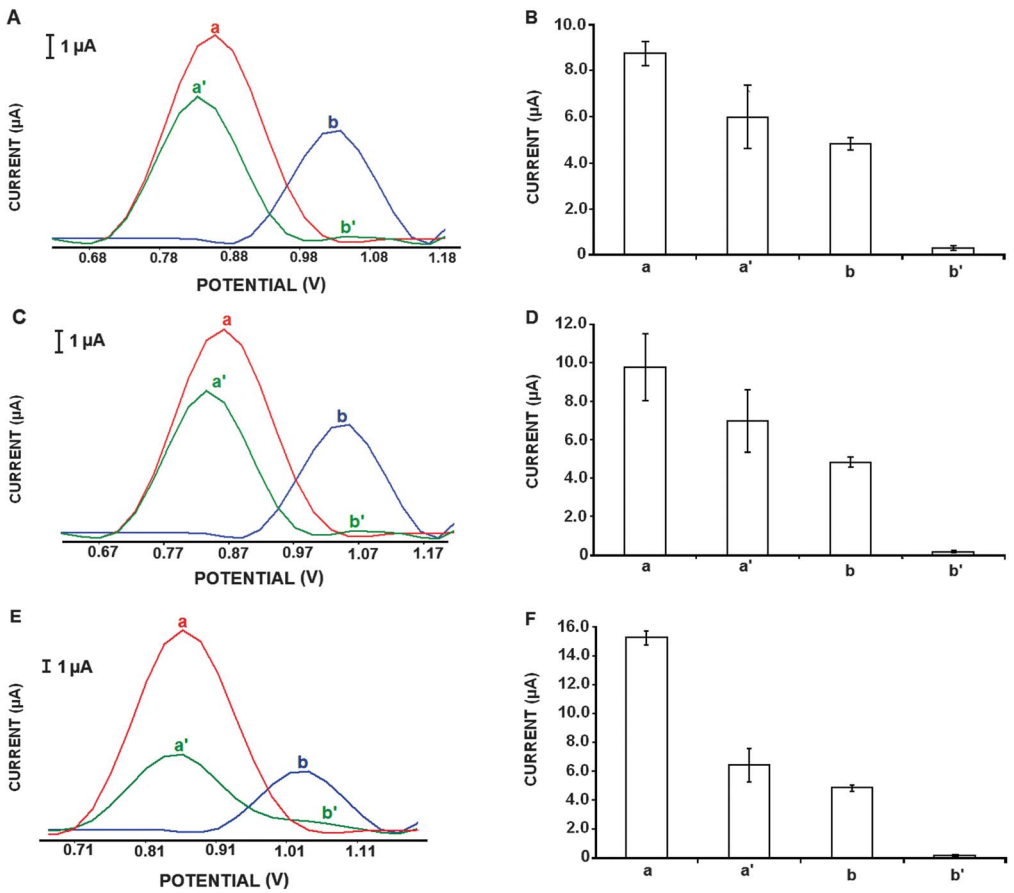


**Fig. 5** (A), (C), (E) DPVs and (B), (D), (F) histograms representing MC and guanine oxidation signals observed before and after the interaction of 80 μg $mL^{-1}$ MC with 120 μg $mL^{-1}$ dsDNA using GO-PGEs. (A) and (B) for 7.5 min interaction time; (C) and (D) for 15 min interaction time; (E) and (F) for 30 min interaction time; the oxidation signal of MC: (a) before interaction, (a′) after interaction with dsDNA; and the oxidation signal of guanine: (b) before interaction, (b′) after interaction of MC with dsDNA.

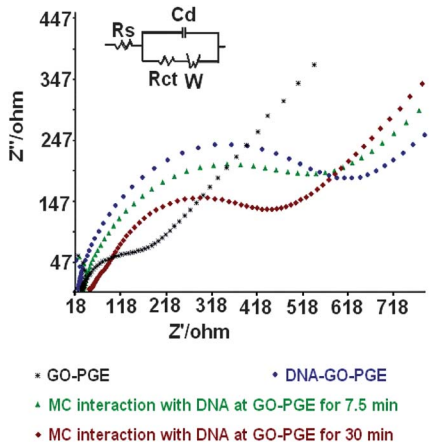


**Fig. 6** Nyquist diagrams recorded at the GO-modified electrode before and after interaction of 80 μg $mL^{-1}$ MC with 120 μg $mL^{-1}$ dsDNA at different interaction times of 7.5 and 30 min. Inset is the equivalent circuit model used to fit the impedance data, the parameters of which are: $R_S$ is the solution resistance; the constant phase element $C_d$ is related to the space charge capacitance at the DNA/electrolyte interface; $R_{ct}$ represents the charge transfer resistance at the DNA/electrolyte interface; the constant phase element $W$ is the Warburg impedance due to mass transfer to the electrode surface.

which are formed specifically at CpG and GpG base pairs of dsDNA. In agreement with earlier studies performed using different electrochemical transducers (CSPE, CPE and HMDE[38–40,44]), similar damage is expected to occur at the oxidizable groups of the guanine base due to the biointeraction process between MC and dsDNA on our electrodes.

In our study, the guanine peak magnitude was also used as the transduction signal for recognizing the DNA interacting agent, MC. As a result of MC interaction with dsDNA, a decrease in the guanine signal was obtained (Fig. 5). DNA modifications were estimated based on the value of the percentage of guanine peak height change ($S$%),[50] which is the ratio of the guanine peak height after the interaction ($S_s$), and the guanine peak height before the interaction ($S_b$):

$$S\% = (S_s/S_b) \times 100$$

Thus, the DPV signal of the sensor in the absence of the analyte served as a 'blank', or 100%. Conventionally, if a sample had an $S > 85\%$ it was considered not to be toxic, whereas if it had an $S$% between 50 and 85 was considered moderately toxic and if it had an $S < 50\%$ was considered toxic.[50] Using the equation given above, the values of $S$% were calculated for 7.5, 15 and 30 min, and were found to be 5.7, 3.3, and 2.8% respectively. Based on these calculated $S$% values, MC can be considered as a toxic chemical.

In accordance with the reference method of Ozkan *et al.*,[38] the partition coefficient of MC on the surface of the GO-modified electrode was estimated from the results presented in Fig. 5 by the following equation:

$$\text{Partition coefficient} = MC_{bound}/MC_{free} = |(i_{bound} - i_{free})/i_{free}|$$

where $i_{free}$ is the oxidation peak current of MC obtained before and $i_{bound}$ is the oxidation peak current of MC obtained after interaction with dsDNA. In agreement with this work,[38] the partition coefficient for 80 μg $mL^{-1}$ MC was found to be 0.31 and 0.58 for 7.5 and 30 min interaction times, respectively.

Based on three repetitive voltammetric measurements employing solutions of 80 μg $mL^{-1}$ MC and 120 μg $mL^{-1}$ dsDNA the mean response of the MC and guanine oxidation signals were calculated as 5850 ± 824.72 nA and 188 ± 52 nA respectively and the detection limit ($S/N = 3$) was estimated as 1.39 μg $mL^{-1}$ which is comparable to the values reported in earlier works.[41,44,51] With respect to the electrode modification approach, a simpler and faster modification step was used herein for the development of disposable GO-modified electrodes by following passive adsorption. In addition, a smaller amount of nucleic acid was employed compared to the electrodes modified with poly(vinylferrocenium) ($PVF^+$),[40] or single-walled carbon nanotube (SWCNT)/$PVF^+$,[52] prepared electrochemically by potential-controlled coulometry technique.

EIS was used to probe the various steps on the construction of the sensor. Following GO modification, the average $R_{ct}$ value was calculated as 178 Ω (shown in Fig. 6), which is larger than the one obtained by the unmodified one (not shown). The change of the $R_{ct}$ value after modification was strong proof that GO had been immobilized on the electrode surface. A further increase of the $R_{ct}$ values was obtained after dsDNA immobilization onto the surface of the GO-modified electrode as a result of the enhanced resistance to the charge-transfer at the electrode surface. The negatively charged phosphate backbone of dsDNA prevented the redox couple, $[Fe(CN)_6]^{3-/4-}$, from reaching the electrode surface, leading to an almost 3.5 times larger $R_{ct}$ value (Fig. 6). The surface-confined interaction of the anticancer drug MC with dsDNA at different interaction times, *e.g.* 7.5 and 30 min, led to a decrease in the $R_{ct}$ value by 7.1% and 20.5% respectively. The interaction of MC with the double helix form of DNA at the electrode surface should decrease the negative charge present on the electrode surface, thus reducing the resistance the charge transfer. Consequently, the EIS results complemented successfully the voltammetric results for monitoring this biomolecular recognition process.

## 4. Conclusion

Through this work we report for the first time that GO-modified PGEs can yield a rapid and sensitive route for the detection of nucleic acids (dsDNA) and drugs, using as model system the anticancer drug MC. Easy surface modification of PGE with GO was performed herein using smaller amounts of nucleic acids to develop single-use GO-modified DNA sensors compared to the earlier advanced DNA sensors modified using $PVF^+$,[40] or SWCNT/$PVF^+$.[52]

A signal enhancement of 21.4% and 34.4% was obtained for MC and guanine respectively by using GO-modified disposable electrodes in comparison with the unmodified ones due to the fact that the GO provides a higher surface area at the electrode surface for the binding of drug, or nucleic acids.

Additionally, the GO-based sensor technology was demonstrated for the sensitive electrochemical detection of the biomolecular interaction process between MC and dsDNA. The high decreases in both signals of MC and guanine were recorded as 31.3–58.1% for MC, and 94.3–97.2% for guanine after the

 

interaction process at the surface of the GO-modified electrode in different interaction times of 7.5 and 30 min.

As a conclusion, single-use GO-modified electrodes developed for monitoring biorecognition processes have presented many advantages: being easy to use, cost-effective, enabling rapid detection with good repeatability in comparison to the conventional electrodes, *e.g.*, CPE, glassy carbon electrode, CSPE, HMDE, gold electrode and advanced ones modified using conductive polymers and carbon nanotubes.

## Acknowledgements

This work was supported by the Royal Society through Joint Project Scheme (Project No. 1212R0168). A.E. acknowledges the Turkish Academy of Sciences (TUBA) as an Associate member for its partial support. Authors would like to thank Dr. M. McMullan for the assistance on the synthesis of graphene oxide.

## References

1 D. E. Thurston, *Br. J. Cancer*, 1999, **80**, 65–85.
2 J. Wang and A. Review, *Electroanalysis*, 2005, **17**, 7–14.
3 A. Erdem, *Talanta*, 2007, **74**, 965–974.
4 E. Palecek and M. Fojta, *Anal. Chem.*, 2001, **73**, 75A–83A.
5 A. Erdem, B. Kosmider, R. Osiecka, E. Zyner, J. Ochocki and M. Ozsoz, *J. Pharm. Biomed. Anal.*, 2005, **38**, 645–652.
6 I. Haq, H. E. Ladbury, B. Z. Chowdhry, T. C. Jenkins and J. B. Chaires, *J. Mol. Biol.*, 1997, **271**, 244–257.
7 E. Gavathiotis, G. J. Sharman and M. S. Searle, *Nucleic Acids Res.*, 2000, **28**, 728–735.
8 P. Colson, C. Bailly and C. Houssier, *Biophys. Chem.*, 1996, **58**, 125–140.
9 R. Krautbauer, L. H. Pope, T. E. Schrader, S. Allen and H. E. Gaub, *FEBS Lett.*, 2002, **510**, 154–158.
10 M. Song, R. Zhang and X. Wang, *Mater. Lett.*, 2006, **60**, 2143–2147.
11 V. Brabec, *Electrochim. Acta*, 2000, **45**, 2929–2932.
12 M. Catalán, A. Á. Lueje and S. Bollo, *Bioelectrochemistry*, 2010, **79**, 162–167.
13 F. Jelen, A. Erdem and E. Palecek, *Bioelectrochemistry*, 2002, **55**, 165–167.
14 A. Erdem and M. Ozsoz, *Anal. Chim. Acta*, 2001, **437**, 107–114.
15 S. Krizkova, V. Adam, J. Petrlova, O. Zitka, K. Stejskal, J. Zehnalek, B. Sures, L. Trnkova, M. Beklova and R. Kizeka, *Electroanalysis*, 2007, **19**, 331–338.
16 A. Erdem, H. Karadeniz and A. Caliskan, *Electroanalysis*, 2009, **21**, 464–471.
17 H. Heli, M. Zarghan, A. Jabbari, A. Parsaei and A. A. Moosavi-Movahedi, *J. Solid State Electrochem.*, 2010, **14**, 787–795.
18 E. Yapasan, A. Caliskan, H. Karadeniz and A. Erdem, *Mater. Sci. Eng., B*, 2010, **169**, 169–173.
19 A. Caliskan, H. Karadeniz, A. Meric and A. Erdem, *Anal. Sci.*, 2010, **26**, 117–120.
20 H. Karadeniz, G. Armagan, A. Erdem, E. Turunc, A. Caliskan, L. Kanit and A. Yalcin, *Electroanalysis*, 2009, **21**, 2468–2476.
21 J. Wang, A. Kawde, A. Erdem and M. Salazar, *Analyst*, 2001, **126**, 2020–2024.
22 M. R. P. Querioz, E. M. S. Castanheira, M. S. D. Carvalho, A. S. Abreu, P. M. T. Ferreira, H. Karadeniz and A. Erdem, *Tetrahedron*, 2008, **64**, 382–391.
23 A. K. Geim and K. S. Novoselov, *Nat. Mater.*, 2007, **6**, 183–191.
24 D. A. C. Brownson and C. E. Banks, *Analyst*, 2010, **135**, 2768–2778.
25 C. Stampfer, E. Schurtenberger, F. Molitor, J. Guttinger, T. Ihn and K. Ensslin, *Nano Lett.*, 2008, **8**, 2378–2383.
26 D. Li and R. B. Kaner, *Science*, 2008, **320**, 1170–1171.
27 N. M. R. Peres, F. Guinea and A. H. Castro Neto, *Phys. Rev. B: Condens. Matter Mater. Phys.*, 2006, **73**, 125411–125434.
28 O. Leenaerts, B. Partoens and F. M. Peeters, *Phys. Rev. B: Condens. Matter Mater. Phys.*, 2008, **77**, 125416–125422.
29 B. Huang, Z. Li, Z. Liu, G. Zhou, S. Hao, J. Wu, B. Gu and W. H. Duan, *J. Phys. Chem. C*, 2008, **112**, 13442–13446.
30 P. K. Ang, W. Chen, A. T. S. Wee and K. P. Loh, *J. Am. Chem. Soc.*, 2008, **130**, 14392–14393.
31 N. Shang, P. Papakonstantinou, M. McMullan, M. Chu, A. Stamboulis, A. Potenza, S. S. Dhesi and H. Marchetto, *Adv. Funct. Mater.*, 2008, **18**, 3506–3514.
32 F. Yang, K. J. Huang, D. J. Niu, C. P. Yang and Q. S. Jing, *Electrochim. Acta*, 2011, **56**, 4685–4690.
33 S. Alwarappan, A. Erdem, C. Liu and C. Z. Li, *J. Phys. Chem. C*, 2009, **113**, 8853–8857.
34 Y. R. Kim, S. Bong, Y. J. Kang, Y. Yang, R. K. Mahajan, J. S. Kim and H. Kim, *Biosens. Bioelectron.*, 2010, **25**, 2366–2369.
35 M. Muti, S. Sharma, A. Erdem and P. Papakonstantinou, *Electroanalysis*, 2011, **23**, 272–279.
36 W. Szybalski and V. N. Iyer, *Fed. Proc., Fed. Am. SOC. Exp. Biol.*, 1964, **23**, 946–957.
37 R. Bizanek, B. F. McGuinness, K. Nakanishi and M. Tomasz, *Biochemistry*, 1992, **31**, 3084–3091.
38 D. Ozkan, H. Karadeniz, A. Erdem, M. Mascini and M. Ozsoz, *J. Pharm. Biomed. Anal.*, 2004, **35**, 905–912.
39 H. Karadeniz, L. Alparslan, A. Erdem and E. Karasulu, *J. Pharm. Biomed. Anal.*, 2007, **45**, 322–326.
40 F. Kuralay, A. Erdem, S. Abacı, H. Ozyoruk and A. Yıldız, *J. Appl. Electrochem.*, 2010, **40**, 2039–2050.
41 P. Perez, C. Teijeiro and D. Marin, *Langmuir*, 2002, **18**, 1760–1763.
42 S. Niyogi, E. Bekyarova, M. E. Itkis, J. L. McWilliams, M. A. Hamon and R. C. Haddon, *J. Am. Chem. Soc.*, 2006, **128**, 7720–7721.
43 J. N. Miller and J. C. Miller, *Statistics and Chemometrics for Analytical Chemistry*, Pearson Education, Essex, 4th edn, 2000.
44 D. Marin, P. Perez, C. Teijeiro and E. Palecek, *Biophys. Chem.*, 1998, **75**, 87–95.
45 R. Lipman, J. Weaver and M. Tomasz, *Biochim. Biophys. Acta, Nucleic Acids Protein Synth.*, 1978, **521**, 779–791.
46 D. J. Kaplan and L. H. Hurley, *Biochemistry*, 1981, **20**, 7572–7580.
47 J. Portugal and F. J. Sanchez-Baeza, *Biochem. J.*, 1995, **306**, 185–190.
48 J. Weaver and M. Tomasz, *Biochim. Biophys. Acta*, 1982, **697**, 252–254.
49 M. M. Paz, A. Das and M. Tomasz, *Bioorg. Med. Chem.*, 1999, **7**, 2713–2726.
50 G. Bagni, D. Osella, E. Sturchio and M. Mascini, *Anal. Chim. Acta*, 2006, **573**, 81–89.
51 D. Marin, P. Perez, C. Teijeiro and E. Palecek, *Anal. Chim. Acta*, 1998, **358**, 45–50.
52 E. Canavar, F. Kuralay and A. Erdem, *Electroanalysis*, 2011, **23**, 2343–2349.